

# Influence of System Integration and Packaging on Its Inductive Power Link for an Integrated Wireless Neural Interface

Sohee Kim\*, *Member, IEEE*, Reid R. Harrison, *Member, IEEE*, and Florian Solzbacher, *Member, IEEE*

**Abstract**—In an integrated wireless neural interface based on the Utah electrode array, the implanted electronics are supplied with power through inductive coupling between two coils. This inductive link is affected by conductive and dielectric materials and media surrounding the implant coil. In this study, the influences of the integration of an implant coil on a silicon-based IC and electrode array, thin-film Parylene-C encapsulation, and physiological medium surrounding the coil were investigated systematically and quantitatively by empirical measurements. A few embodiments of implant coils with different geometrical parameters were made with a diameter of  $\sim 5.5$  mm by winding fine wire with a diameter of approximately  $50 \mu\text{m}$ . The parasitic influences affecting the inductive link were empirically investigated by measuring the electrical properties of coils in different configurations and in different media. The distance of power transmission between the transmit and receive coils was measured when the receive coil was in air and immersed in phosphate buffered saline solution to simulate an implanted physiological environment. The results from this study quantitatively address the influences of factors such as device integration, encapsulation, and implantation on its inductive power link, and suggest how to maximize the efficiency in power transmission for such neural interface devices powered inductively.

**Index Terms**—Coil, inductive coupling, integration, neural interface, packaging, quality factor, resonance frequency, Utah electrode array (UEA).

## I. INTRODUCTION

RECENTLY, an integrated wireless neural interface device based on the Utah electrode array (UEA) has been developed, which is intended for chronic neural signal recording [1]–[4]. The implanted electronics in this device are supplied with power through inductive coupling between two coils. The power receive coil was previously micromachined in a flat spiral configuration using thin-film technology [5] and integrated with other active and passive components consisting of this neural

interface [4]. When such a neural interface is implanted in the body, the inductive power link is affected by the conductive and dielectric properties of the materials and media present between an external power transmit coil and an implanted power receive coil. The following factors would affect the inductive power link due to the conductive and dielectric properties of the materials and media surrounding the implant coil and present between them:

- 1) the silicon substrate underneath the implant coil when the coil is integrated with silicon-based IC and UEA [3], [4];
- 2) the coating materials used for device encapsulation [6]–[8];
- 3) the surrounding biological medium in a physiological environment.

Practically, tuning a power receive coil at a specific frequency to maximize the voltage and power reception for such implantable microdevices can be difficult because the presence of conductive and/or dielectric media nearby the coil will affect the coil's electrical property, and as a result, its performance in wireless power reception. Therefore, it is important to predict changes in electrical properties of the coil caused by device integration, encapsulation, and implantation in a physiological environment in advance, in order to achieve a maximum power transmission distance. This paper presents the quantitative investigation of these effects for an implantable neural interface device on its wireless power link by empirical measurements.

Fig. 1 presents an example of the integrated neural interface device with an overall dimension of  $7.6 \times 8.0 \times 2.5$  mm, including the electrodes. For use in such neural interfaces, two embodiments of flat spiral coils were built with a diameter of up to 5.5 mm, by winding insulated Cu and Au wires with a diameter of approximately  $50 \mu\text{m}$ . To quantitatively investigate the aforementioned influences of the materials and media surrounding the coil on its power transmission, the electrical properties of the coils such as inductance, series resistance, and capacitance were measured with coils in different configurations. By observing the change in impedance of coils in different configurations and different media, the influence of each material and medium surrounding the coil could be quantitatively determined. The distance of power transmission between the transmit and receive coils was measured and compared for coils in different configurations.

Although there have been a body of publications investigating the material properties of polymeric encapsulants for implantable devices including not only Parylene-C that is used in

Manuscript received August 6, 2008; revised March 11, 2009. First published August 18, 2009; current version published November 20, 2009. This work was supported in part by the National Institute of Health/National Institute of Neurological Disorders and Stroke, Neural Prosthesis Program under Contract HHSN265200423621C and in part by the Defense Advanced Research Projects Agency, Revolutionizing Prosthesis 2009 Program under Contract N66001-06-C-8005. Asterisk indicates corresponding author.

\*S. Kim was with the Department of Electrical and Computer Engineering, University of Utah, Salt Lake City, UT 84112 USA. She is now with the Department of Mechatronics, Gwangju Institute of Science and Technology, Gwangju 500-712, Korea (e-mail: soheekim@gist.ac.kr).

R. R. Harrison and F. Solzbacher are with the Department of Electrical and Computer Engineering, University of Utah, Salt Lake City, UT 84112 USA (e-mail: r.harrison@ece.utah.edu; florian.solzbacher@utah.edu).

Color versions of one or more of the figures in this paper are available online at <http://ieeexplore.ieee.org>.

Digital Object Identifier 10.1109/TBME.2009.2028614

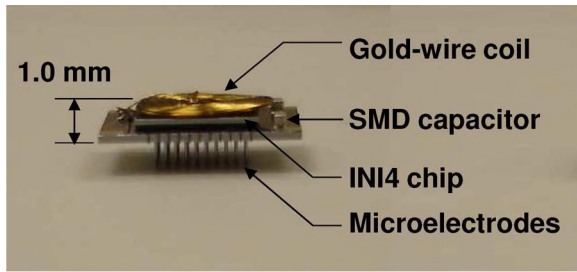


Fig. 1. Photograph of an integrated neural interface. The dimensions are 7.6 mm  $\times$  8.0 mm, with an overall height of 2.5 mm including the electrodes.

this study, but also epoxies, polyimides, silicones, or inorganic materials such as silicon nitride and silicon carbide [6]–[20], most of these publications have not dealt with the effect of encapsulation materials on inductive link for a wirelessly operating device. This study focuses on the influence of device encapsulation on the resonance frequency and quality factor of the implant coil, and its subsequent use in wireless power transmission by systematic empirical measurements.

## II. MATERIALS AND METHODS

### A. Design of Implant Coils and Test Assemblies

In our application, an inductance of 20–30  $\mu$ H was desirable for the implant coil to match the input impedance of the implant IC and to achieve a sufficient quality factor [21]. The quality factor was desired to be greater than 14, including all parasitic losses. The outer diameter of the coil was determined to be within 5.5 mm to fit the overall dimensions of the neural interface [4]. After a series of numerical simulations using finite element analysis (FEA) [23], optimized coil designs were derived and sample coils were made by winding microwires at IEC Company (Conway, SC). We made two embodiments of microwire wound coils: one was made of insulated Cu wire with a diameter of 44.7  $\mu$ m and the other was made of Au wire with a diameter of 55.9  $\mu$ m. The wire insulation material was solderable polyester (trade name: Terasod, MW-77) that has a temperature rating of 180  $^{\circ}$ C, and the insulation thickness was 5.1  $\mu$ m minimum and 7.6  $\mu$ m maximum. Due to the process to integrate the coils on the UEA devices, which was a soldering or a wire bonding process, a material providing solderability/bondability was preferred as wire insulation. Both types of coils had three-layer flat spiral shape. Cu coils had a coil diameter of 5.0 mm, 34 turns per layer, and a coil thickness of 160  $\mu$ m, while Au coils had a coil diameter of 5.5 mm, 30 turns per layer, and a coil thickness of 200  $\mu$ m. Cu wire wound coils were intended for bench top, *in vitro*, and acute *in vivo* tests of supplying the integrated neural interface, while Au wire coils were to be integrated in the devices for chronic implantation. The design parameters used for the implant coils are listed in Table I.

The effects of coil integration on the IC/UEA, Parylene-C encapsulation, and implantation in a physiological environment were investigated by measuring the impedance of coils in different configurations. Each type of coil was prepared in three different configurations, as depicted in Fig. 2: the coil in isolation

TABLE I  
DESIGN PARAMETERS OF TWO TYPES OF MICROWIRE WOUND COILS

	Cu-wire coil	Au-wire coil
Outer diameter	5.0 mm	5.5 mm
Inner diameter	1.3 mm	1.3 mm
Wire diameter	44.7 $\mu$ m	55.9 $\mu$ m
Number of turns	34 per layer	30 per layer
Coating thickness	5 $\mu$ m	5 $\mu$ m
Thickness	165 $\mu$ m (3 layers)	200 $\mu$ m (3 layers)
Electrical conductivity	$5.9 \times 10^7$ S/m	$4.5 \times 10^7$ S/m

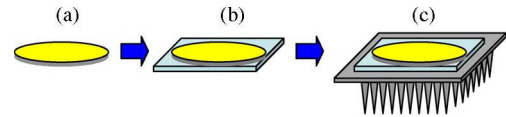


Fig. 2. Coil assemblies to investigate the influence of conductive silicon-based substrates. (a) Coil. (b) Coil on IC. (c) Coil on IC and array.

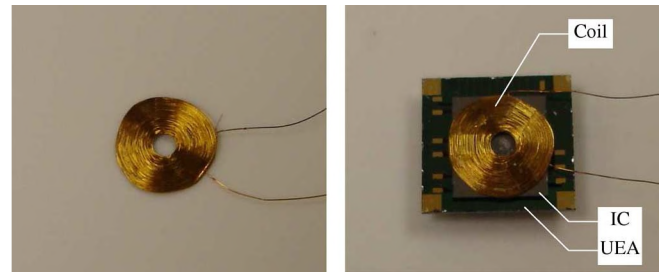


Fig. 3. (Left) Photograph of a flat three-layer Au wire wound coil in isolation, and (right) when mounted on the IC and the UEA.

(assembly A), the coil on an IC (assembly B), and the coil on an IC and UEA (assembly C) by using adhesive glue. Fig. 3 shows photographs of the sample assemblies. The IC used in this study was referred to as “INI4” (INI for “integrated neural interface,” 4: version number), and includes circuits for 100 neural signal amplifiers, data processing, power and clock recovery, and an RF transmitter for data telemetry [24]–[27]. The INI4 chips were fabricated by X-FAB Semiconductor (Erfurt, Germany) in a 0.6- $\mu$ m 3M2P BiCMOS process, and had dimensions of 4.9  $\times$  5.6 mm with a thickness of 380  $\mu$ m. The impedance of coils in assemblies A, B, and C was measured over a frequency range of 75 kHz–30 MHz, by using a precision LCR meter (Agilent 4285A, Santa Clara, CA). The precision LCR meter was calibrated in open- and short-circuit configurations when an adapter board was attached, prior to coil measurements. The coils were modeled as a combination of series inductance ( $L_s$ ) and series resistance ( $R_s$ ).

Prior to assembling the coil with the IC and UEA, the coil assembly A (see Fig. 2) was tuned to resonate at a specific frequency by adding a capacitance in parallel to the coil. An operating frequency of 2.765 MHz was chosen to transmit power, clock and command data to the INI4 chip for our application. This choice was made due to low tissue absorption in the 1–10 MHz range, the need for a 345.6 kHz clock on the chip, which is easily achieved by dividing the power frequency by 8, and a moderate quality factor at the chosen frequency that was

anticipated for the dimension and design of the used coils. The capacitance was optimized to tune the coil assembly A at 2.765 MHz  $\pm$  5 kHz, and this optimized capacitance was used for all other coil assemblies and configurations: assemblies B and C, assembly C encapsulated with Parylene-C layer, and immersed in physiological solution.

### B. Parylene Encapsulation

A thin-film Parylene-C layer was used to provide conformal encapsulation for the entire neural interface device, since the device contains electronic components such as very large-scale integrated (VLSI) INI4 chip and a few discrete components that are exposed to the physiological environment, and therefore, requires insulation from the environment. An adhesion promoter, 0.5% Silquest A-174 silane (GE Silicones, Friendly, WV), was applied to the coil assembly C (see Fig. 2) prior to Parylene-C deposition. Parylene-C film was deposited using a Paratech 3000 Labtop Deposition System (Paratech Coating, Inc., Aliso Viejo, CA) by chemical vapor deposition (CVD). Parylene-C dimer precursor was acquired from Cookson Electronics Equipment, USA. The dimer sublimation temperature was controlled between 120 °C and 170 °C to keep the vapor pressure constant until the dimer sublimated completely. The sublimation rate was estimated from the vapor pressure curve to be  $\sim$ 0.03 g/min. The dimer vapor was subsequently pyrolyzed into reactive monomers at 670 °C. The devices were placed in the deposition chamber at room temperature and pumped down to a base pressure  $<$ 10 mtorr before sublimation of the Parylene dimer. The Parylene-C acts as a biocompatible layer that protects the device from ions in physiological environments. The detailed material properties and encapsulation characteristics of Parylene-C are described elsewhere [7], [8] and will not be discussed in this paper.

To investigate the influence of Parylene encapsulation for the entire device (assembly C, see Fig. 2) and the surrounding physiological medium on the electrical properties of the coils, the coils' impedance, series inductance, and resistance were measured and compared for assembly C in different configurations: before Parylene coating, after Parylene coating, and when immersed in phosphate buffered saline (PBS) solution. Two Cu wire coils were used to investigate the influence of Parylene encapsulation layer over the power receive coil. One Cu coil (assembly C) was coated with Parylene and the other was not coated. The impedance of both coils was measured in the air and when immersed in PBS solution. For the latter, the coil was immersed in PBS filled in a Petri dish with a diameter of 10 cm. The thickness of the PBS solution present above the coil was 5 mm.

### C. Power Transmission

The power transmit coil used in this study was a planar spiral coil printed on a circuit board [26], which had an outer diameter of 5.8 cm, an inner diameter of 0.9 cm, and 28 turns, as shown in Fig. 4, resulting in an inductance of 21  $\mu$ H and series resistance of 5.1  $\Omega$ . Previous simulation studies indicated that a coil of this size optimizes the coil coupling coefficient  $k$  for an implantable



Fig. 4. Power and command transmitter with an integrated PCB coil in a diameter of 5.8 cm. The coil is driven at 2.765 MHz to provide power and a clock signal to the INI4 chip, and the amplitude of this signal is modulated to send commands to the chip.

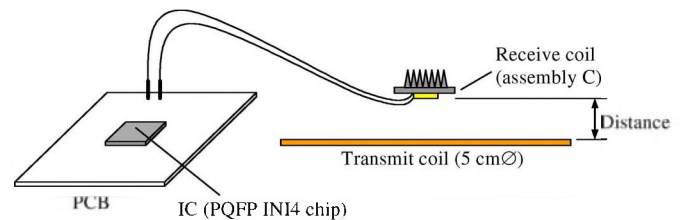


Fig. 5. Schematic of the experimental setup to measure the power transmission distance between the transmit and receive coils. The distance between the two coils is adjustable using glass slides.

coil with a 5.5 mm diameter and a coil-to-coil spacing in the range of 1.5–2.0 cm, as we expect in implanted cortical applications [21], [22]. The intended application targets at the distance between the external transmit coil and implanted receive coil to be greater than the thickness of the tissue in between. This minimum coil distance was determined based on the consultation with a neurosurgeon [22]. Also, the distance between the coils needs to be limited so that exposing the implanted tissue to an unnecessarily large magnetic field can be avoided. The power board used a class E power amplifier to create a 2.765-MHz ac waveform of up to 80 V<sub>rms</sub> from a 10 V dc supply. The resulting ac magnetic field was received at the implant coil and supplied the IC connected to the coil. Techniques described in [21] were used to optimize the power link. The power transmitter board drew a current of 220 mA from the 10 V dc supply, resulting in a power consumption in the entire transmitter circuitry of 2.2 W. The voltage and current measured at the transmit coil were up to 80 V<sub>rms</sub> and 0.39 A<sub>rms</sub>, respectively. The setup to measure the received voltage at the implant coil is depicted in Fig. 5. The receive coil was placed above the transmit coil, with center points aligned. The distance between the two coils was adjusted using 1 mm-thick glass slides. The receive coil was connected to a surface mount device (SMD) packaged INI4 chip that was mounted on a printed circuit board (PCB), through lead wires in a length of about 4 cm for testing convenience, as shown in Fig. 5. The distance of power transmission was measured for both Cu wire and Au wire coils by measuring the received voltage at the INI4 chip using an oscilloscope (Tektronix TDS 3054B, Beaverton, OR). Because the additional resistances present in the lead wires connecting the coil to the INI4 chip and in the interconnection lines sputter deposited with a



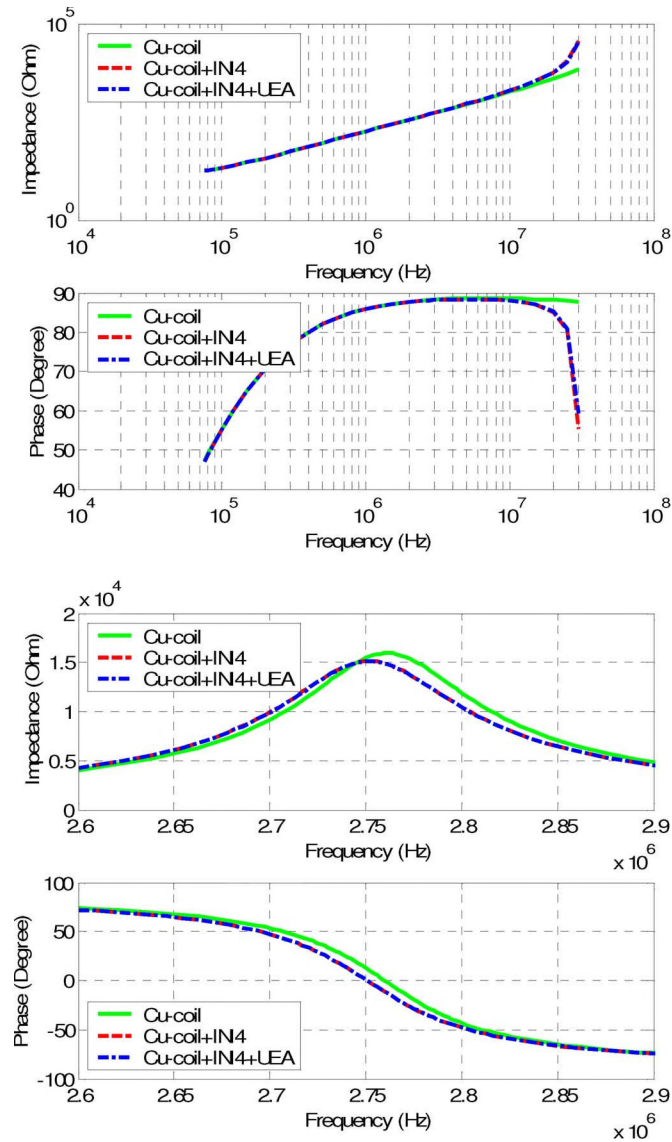


Fig. 6. Measured impedance of a Cu wire coil in assemblies A, B, and C (top) when no external capacitance was used and (bottom) when an external capacitance of 114.6 pF was used to tune the assembly A at 2.765 MHz. This capacitance was used for all other assemblies.

thin-film stack of Ti/Pt/Au on the UEA [4] were not negligible compared to the resistance of the coil itself, the distance of power transmission was measured and compared when these additional resistances were inserted between the coil and the INI4 chip, to model such resistive effects.

### III. RESULTS AND DISCUSSION

#### A. System Integration and Electrical Properties of Coils

The measured impedance of a Cu wire coil is shown in Fig. 6 for assemblies A, B, and C, and the series resistance and inductance for each coil configuration are listed in Table II. The measured impedance of an Au wire coil in different configurations is shown in Fig. 7, and the series resistance and inductance

TABLE II  
ELECTRICAL PROPERTIES OF Cu-WIRE WOUND COIL

	Coil (assembly A)	Coil + IC (assembly B)	Coil + IC + UEA (assembly C)	
$L_s$ ( $\mu\text{H}$ )	At 75 kHz	28.90	28.91	28.91
	At 2.765 MHz	28.98	29.15	29.14
$R_s$ ( $\Omega$ )	At 75 kHz	12.59	12.67	12.66
	At 2.765 MHz	15.30	16.28	16.31
Coil connected w/ a capacitance ( $C_{\text{ext}}=114.6$ pF)	$f_{\text{res}}$ (MHz)	2.761	2.752	2.752
	$C_{\text{coil}}$ (pF)	0.4	1.1	1.1
	$Q$	32.10	30.14	30.14

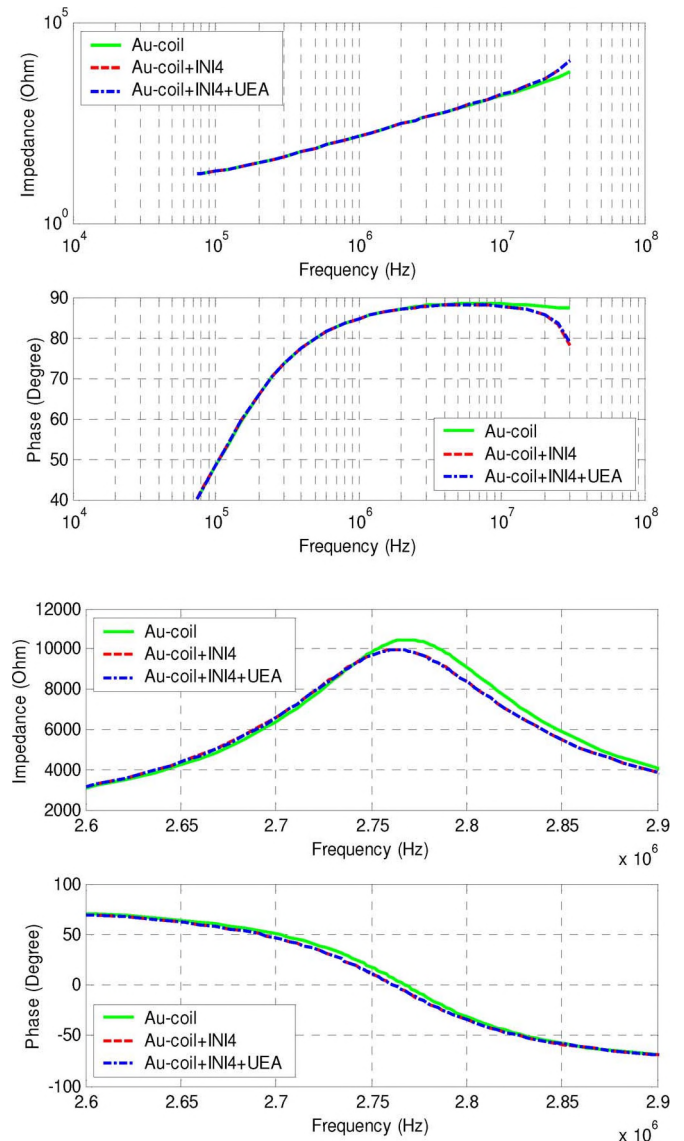


Fig. 7. Measured impedance of a Au wire coil in assemblies A, B, and C (top) when no external capacitance was used and (bottom) when an external capacitance of 140.7 pF was used to tune the assembly A at 2.765 MHz. This capacitance was used for all other assemblies.

are listed in Table III. By comparing the results for assemblies A and B, the integration of the Cu coil on the silicon IC increased the resistance by 6.4% at 2.765 MHz, while it increased the inductance by 0.6%. For the Au coil, the changes in resistance

TABLE III  
ELECTRICAL PROPERTIES OF Au-WIRE WOUND COIL

		Coil (assembly A)	Coil + IC (assembly B)	Coil + IC + UEA (assembly C)
$L_s$ ( $\mu\text{H}$ )	At 75 kHz	23.40	23.41	23.42
	At 2.765 MHz	23.46	23.55	23.55
$R_s$ ( $\Omega$ )	At 75 kHz	13.06	13.02	13.04
	At 2.765 MHz	15.43	16.23	16.28
Coil connected w/ a capacitance ( $C_{\text{ext}}=140.7$ pF)	$f_{\text{res}}$ (MHz)	2.769	2.763	2.763
	$C_{\text{coil}}$ (pF)	0.5	1.1	1.1
	$Q$	25.64	24.45	24.41

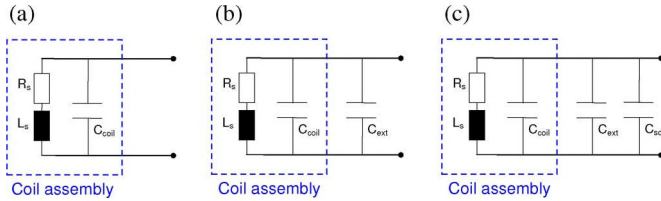


Fig. 8. Equivalent circuit model of a coil in assemblies A, B, and C when (a) no external capacitance was used, (b) an external capacitance was used for resonance, and (c) the coil assemblies were immersed in a physiological solution.

and inductance due to the integration of the coil with the IC were 5.2% and 0.4% at 2.765 MHz, respectively. On the other hand, the influence of the integration of the UEA underneath the IC (compare the results for assemblies B and C) was negligible with changes less than 0.3% in resistance and 0.05% in inductance at 2.765 MHz for both Cu and Au coils. This negligible effect of the integration of highly doped silicon-based UEA on the electrical properties of the coil is due to the fact that the coil is apart from the UEA by the IC in between, with a separation distance of about 430  $\mu\text{m}$  that is sufficiently large so that the coil is not affected by the conductive and dielectric properties of the UEA.

After measuring the impedance of the coil assembly A (see Fig. 2), it was tuned to the frequency at which power, command, and clock signals are transferred to the INI4 chip, by using an external capacitance ( $C_{\text{ext}}$ ), as depicted in Fig. 8. The resonance capacitance  $C_{\text{ext}}$  was chosen in such a way that the resonance occurred in the range of  $2.765 \pm 0.005$  MHz using different capacitor values. The resonance capacitances used for each coil assembly A were 114.6 pF for Cu coil and 140.7 pF for Au coil. The impedance and resonance frequency of the coil assembly A were measured with this optimized capacitance connected in parallel, and compared to those for the assemblies B and C, as shown in Table II for Cu coil and Table III for Au coil. The integration of the coil on the IC shifted the resonance frequency to the lower side by 0.3% (0.009 MHz) for Cu coil and 0.2% (0.006 MHz) for Au coil. The shift in resonance frequency can be explained by the increase in coil capacitance ( $C_{\text{coil}}$  in Fig. 8) due to the integration of the semiconductive IC underneath the coil. The coil capacitance  $C_{\text{coil}}$  was calculated using the equation of

$$C_{\text{coil}} = \frac{1}{(2\pi f_{\text{res}})^2 L_s} - C_{\text{ext}} \quad (1)$$

where  $f_{\text{res}}$  is the measured resonance frequency,  $L_s$  is the measured inductance, and  $C_{\text{ext}}$  is the external capacitance used to tune the coil assembly A. The calculated coil capacitance  $C_{\text{coil}}$  is listed in Table II for Cu coil and Table III for Au coil. This indicates that the integration of the coil and IC increased the coil capacitance by about 0.7 pF for both Cu and Au coils. On the other hand, the integration of the coil on the IC decreased the coil's quality factor  $Q$  by 6.1% for Cu coil and 4.6% for Au coil.

From the results of Figs. 6 and 7, or Tables II and III, the integration of the UEA underneath the coil/IC assembly did not affect the electrical properties of the coil, the resonance frequency, or the  $Q$ .

### B. Polymer Encapsulation and Surrounding Medium on Electrical Properties of Coils

Next, we investigated the influence of Parylene encapsulation of the assembly C (see Fig. 2) and the surrounding physiological medium on the electrical properties of the coil. The impedance, inductance, and resistance of the coils were measured and compared in different configurations: before Parylene coating, after Parylene coating, and when immersed in PBS solution. Here, two Cu wire coils were used to investigate the influence of Parylene encapsulation over the characteristics of the power receive coil. One Cu coil (assembly C) was coated with 6.3  $\mu\text{m}$  Parylene and the other was not coated. Impedances of both coils were measured in air and when immersed in PBS solution, and the results are presented in Fig. 9.

From the results in Fig. 9(a), the encapsulation with Parylene layer decreased the resonance frequency by 0.004 MHz (0.15%) and increased the coil capacitance by 0.4 pF. The coil capacitance in assembly C in different media was calculated from the measured resonance frequency  $f_{\text{res}}$ , inductance  $L_s$ , and the used external capacitance  $C_{\text{ext}}$ , as shown in (1). When the coil assembly encapsulated with Parylene was immersed in solution, the resonance frequency was further decreased by 0.029 MHz (1.1%), resulting in an increase in coil capacitance by 2.5 pF. The influence of the Parylene encapsulation and immersion in PBS solution on the coil's  $Q$  was negligible, with a variation in  $Q$  less than 0.2%. On the other hand, the results in Fig. 9(b) for the coil assembly that was not encapsulated with Parylene presented that the immersion in solution decreased the resonance frequency by 0.334 MHz (12.1%), increasing the coil capacitance by 33.4 pF. The  $Q$  decreased by 56.7% when the coil assembly was immersed in solution. The results in Fig. 9 demonstrate that the Parylene encapsulated coil is significantly less affected by the surrounding dielectric and conductive medium than the coil that was not coated, which indicates that the thin-film polymer encapsulation helps lessen the effect of the surrounding medium on the electrical property of the coil.

The influence of the thickness of Parylene encapsulation was also investigated. Here, Au coil assembly C was used and encapsulated with Parylene in a thickness of 2.9  $\mu\text{m}$ . The measured impedance is shown in Fig. 10. The change in coil's electrical properties due to the 2.9- $\mu\text{m}$  Parylene encapsulation was negligible, while the immersion of the encapsulated coil assembly

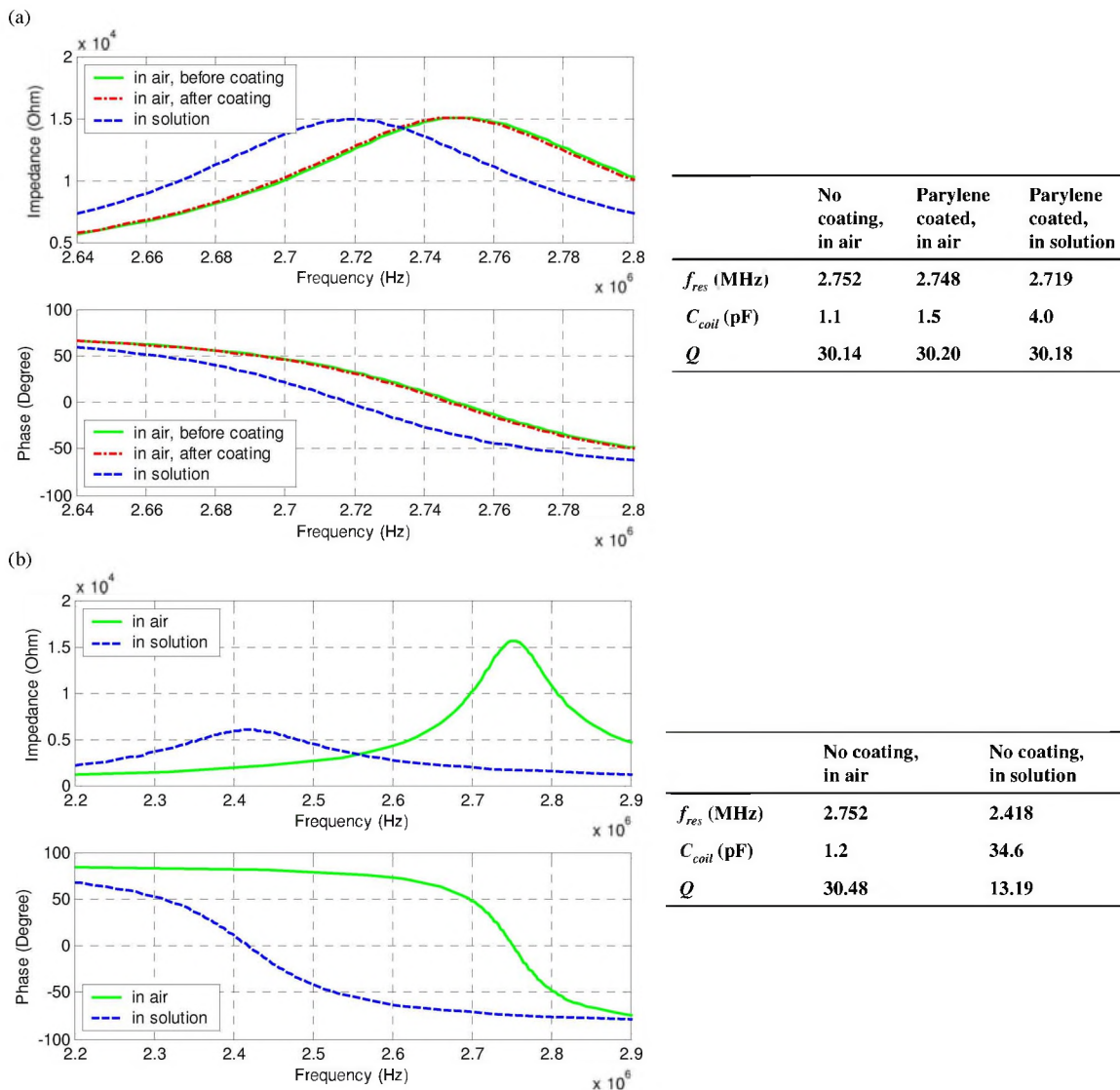


Fig. 9. Measured impedance of a Cu wire coil in assembly C (a) when it was encapsulated with Parylene in a thickness of 6.3  $\mu\text{m}$  and (b) not coated with Parylene. Both coils were measured in air and in PBS solution with the thickness of solution above the coil of 5 mm.

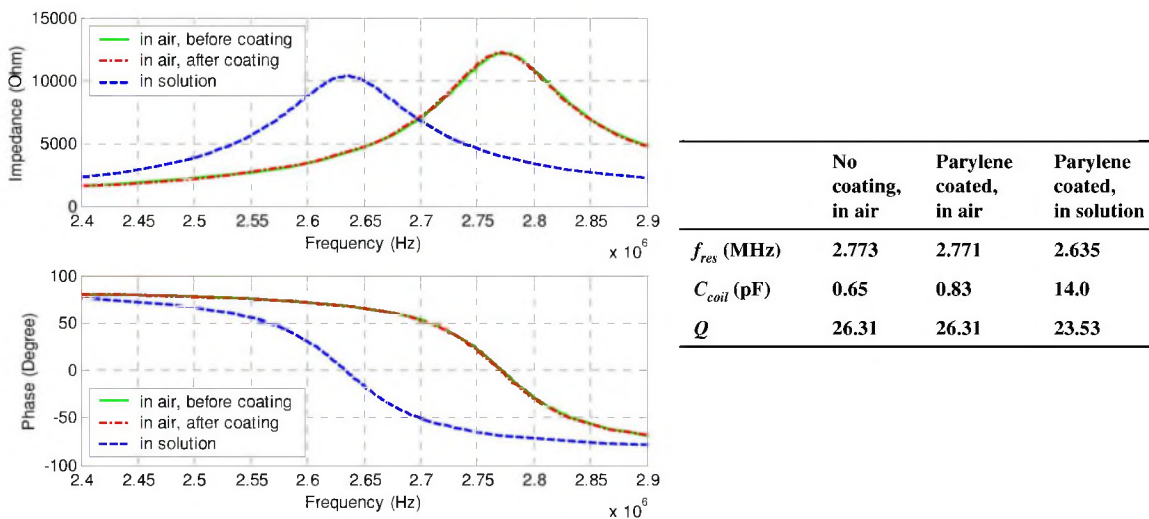


Fig. 10. Measured impedance of an Au wire coil in assembly C encapsulated with Parylene in a thickness of 2.9  $\mu\text{m}$ . The coil assembly was measured in air and in PBS solution with the thickness of solution above the coil of 5 mm.

in PBS solution decreased the resonance frequency by 4.9%, decreased the  $Q$  by 10.6%, and increased the coil capacitance by 13.2 pF. By comparing the results for 6.3  $\mu\text{m}$  Parylene coating in Fig. 9(a) and for 2.9  $\mu\text{m}$  Parylene coating in Fig. 10, the changes in resonance frequency, coil capacitance, and  $Q$  were greater with the coil coated with thinner Parylene layer, although the two coils used in each measurement were not identical geometrically or electrically (see Table I). From the comparison of the results using different Parylene thicknesses (see Figs. 9(a) and 10), the variations due to the presence of physiological medium was about 5% in resonance frequency for a coil coated with 3  $\mu\text{m}$  Parylene, resulting in a decrease in coil impedance to one-third of the value when no physiological medium is present (see Fig. 10), while 1% decrease in resonance frequency for a coil coated with 6  $\mu\text{m}$  Parylene, resulting in a decrease in coil impedance at the intended resonance frequency around 2.76 MHz by 20% [see Fig. 9(a)], which is well within a tolerable range. To minimize such effects of physiological medium on inductive links, the following approaches can be considered: 1) select the SMD capacitor for coil resonance to be smaller than the derived capacitance value when no effect of surrounding medium is taken into account, by the amount corresponding to the predicted change in resonance frequency (for example, about 10% smaller capacitance is needed corresponding to 5% change in resonance frequency for the coil coated with 3  $\mu\text{m}$  Parylene and 3% smaller capacitance corresponding to 1% decrease in resonance frequency for the coil coated with 6  $\mu\text{m}$  Parylene) or 2) increase the Parylene thickness so that the effect of surrounding medium is less significant or negligible. As the former approach is more challenging to convey variations in properties of implanted tissue, which varies implantation to implantation, and therefore, can easily cause slight variations in resonance frequency, we took the latter approach of coating with a sufficiently thick Parylene that can mitigate the influence of the surrounding medium on the inductive link. For this reason, a Parylene thickness of 6  $\mu\text{m}$  or greater was chosen.

The results in Fig. 9(b) present that the immediate contact of the coil with physiological medium (PBS) significantly detunes the resonance frequency and decreases the  $Q$ . Fig. 8(c) shows the equivalent circuit model of a coil in a physiological medium, which adds additional capacitance  $C_{\text{sol}}$  to the coil capacitance  $C_{\text{coil}}$ . This is largely due to the capacitive effect of the dielectric surrounding medium, for example, the dielectric constant is 80 for water at 20 °C while it is 2.9 for Parylene. The high dielectric constant of PBS solution affects the capacitance of the coil by concentrating the electric field near the coil, and therefore, increasing the coil capacitance, resulting in a lower resonance frequency as well as lower quality factor [23].

To confirm the validity of using PBS solution as an implanted physiological model, additional measurements using dead tissue were performed. The coil assembly was placed in a piece of meat with a thickness of 1 cm on top and 1 cm underneath the coil assembly. The lead wires from the coil for connection to the LCR meter were not covered by the tissue in order to prevent additional capacitive effects to the capacitance formed by the two lead wires. The measured impedance of the coil surrounded by tissue showed that the resonance frequency and quality fac-

tor of the coil were similar to those when surrounded by PBS solution, within a difference in resonance frequency of less than 1% and in quality factor of less than 5%. This confirms that using PBS solution approximated the biological tissue reasonably well. In addition, in all measurements using biological tissue, the change in resonance frequency due to the surrounding tissue was slightly smaller than due to the immersion in PBS, which suggests that using PBS solution as implanted model can be considered more conservative.

### C. Connection of Load to Coil

The influence of the connection of a load, i.e., INI4 chip, to the coil was investigated by measuring the distance of power transmission. The received voltage on the INI4 chip was measured using an oscilloscope, as a function of coil separation. When the unregulated voltage was greater than 4.3 V, the INI4 circuitry was functioning properly, and the on-chip regulator was able to supply the chip with a regulated dc voltage of greater than 3.0 V. The distance of power transmission was measured using Cu and Au coils in assembly C when they were connected to the SMD-packaged INI4 chip through lead wires in a length of about 4 cm, as shown in Fig. 5. Due to the input capacitance of the voltage regulation circuitry of the INI4 chip, the resonance of the coil was detuned when connected to the IC. Fig. 11 presents the measured voltage received on the chip through a Au coil when the coil was tuned without considering the input impedance of the chip and when tuned taking it into account. The transmission distance increased from 12 to 18 mm when the coil was tuned with the load connected to it. The received voltage was maximized using a trimmable capacitor, and the optimized capacitance to tune the coil with the load was 92.0 pF for Au coil and 69.2 pF for Cu coil. This indicates that the connection to the INI4 chip adds a capacitance of 40–50 pF parallel to the coil, which needs to be taken into account when selecting the external capacitance ( $C_{\text{ext}}$ ) for coil resonance. This capacitance value closely matches the calculated and simulated values for the chip.

In the recently demonstrated wireless UEA neural interface, thin-film metal traces sputter deposited with Ti/Pt/Au on the UEA are used to interconnect the coil to the INI chip [4]. These interconnection traces were designed to be as short and wide as possible, in order to achieve as small resistance in them as possible. The resistance  $R$  in these interconnection traces was calculated using

$$\frac{1}{R} = \frac{t_{\text{Ti}}w}{\rho_{\text{Ti}}l} + \frac{t_{\text{Pt}}w}{\rho_{\text{Pt}}l} + \frac{t_{\text{Au}}w}{\rho_{\text{Au}}l} \quad (2)$$

where  $\rho$  is the electrical resistivity of the used metals ( $\rho_{\text{Ti}} = 5.54 \times 10^{-7} \Omega\cdot\text{m}$ ,  $\rho_{\text{Pt}} = 1.06 \times 10^{-7} \Omega\cdot\text{m}$ , and  $\rho_{\text{Au}} = 2.20 \times 10^{-7} \Omega\cdot\text{m}$ ),  $t$  is the thickness of each metal ( $t_{\text{Ti}} = 50 \text{ nm}$ ,  $t_{\text{Pt}} = 150 \text{ nm}$ , and  $t_{\text{Au}} = 300 \text{ nm}$ ), and  $w$  and  $l$  are the width and length of the sputter deposited traces ( $w = 250 \mu\text{m}$  and  $l = 2500 \mu\text{m}$ ). The resistance  $R$  was estimated to be 5  $\Omega$ . As this additional resistance decreases the quality factor of the coil, minimizing this resistance is desired for a high efficiency in power transmission. The equivalent circuit model of the coil



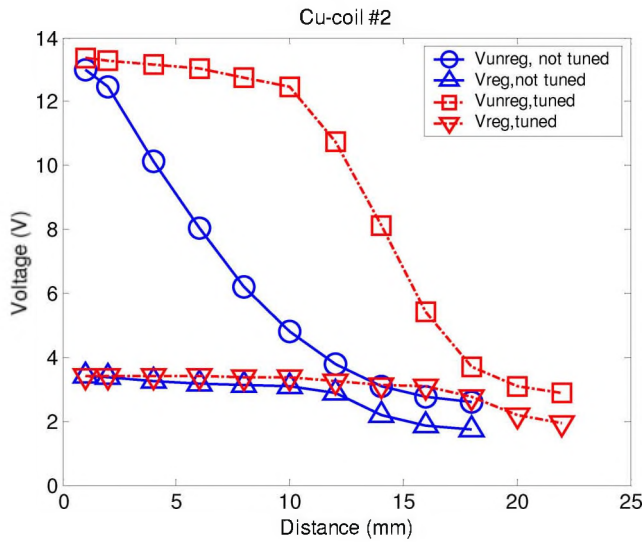
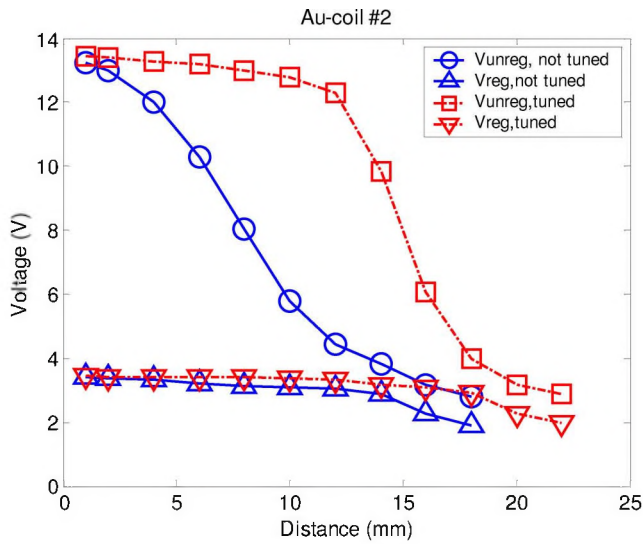


Fig. 11. Measured voltages received at the IN14 chip through (top) Au coil and (bottom) Cu coil when the coils were tuned without considering the load (noted “not tuned” in the plots) and tuned considering the load connected to the coil (noted “tuned” in the plots).

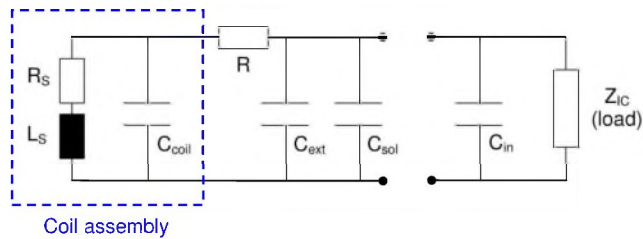


Fig. 12. Equivalent circuit model of a coil including an additional resistance that models the thin-film metallization deposited on the UEA for component interconnection.

including all parasitic effects such as this additional resistance is depicted in Fig. 12. The unregulated voltage at the IC connected to a Au wire coil (assembly C) was measured using the setup as shown in Fig. 5. Fig. 13 presents the measured unregulated voltage received at the IC as a function of coil-to-coil distance and the additional resistance inserted between the coil

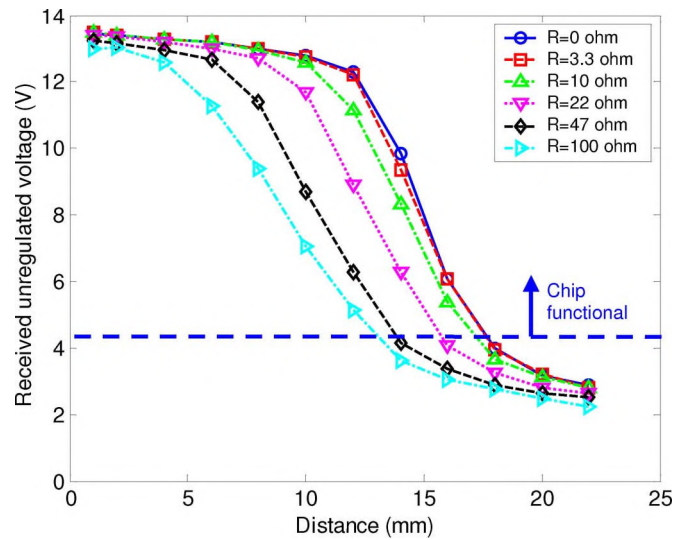


Fig. 13. Measured voltage at the IN14 chip received through Au coil as a function of coil separation, when various resistances  $R$  modeling the thin-film interconnection metallization were used. The IC worked properly when the unregulated voltage was greater than 4.3 V.

and the input of the IN14 chip. When the additional resistance  $R$  was smaller than  $10 \Omega$ , which is double the resistance in the thin film deposited interconnections, the variation in transmission distance was less than about 5%. As  $R$  increased, the transmission distance decreased.

IV. SUMMARY AND CONCLUSION

In this study, the conductive and dielectric effects of the materials and media surrounding an implant coil on the inductive power link were investigated empirically and quantitatively. The integration of the coil on the silicon-based IC had little effect in increasing the resistance and inductance by about 6% and about 0.5% at 2.765 MHz, respectively, while the integration with the UEA did not affect the electrical property of the coil due to the separation between the coil and the UEA. The encapsulation of the device with Parylene had little effect on the electrical property of coils, with changes in both resonance frequency and  $Q$  of less than 0.2%.

On the other hand, the immersion of the coil in physiological solution changed the coil characteristics. When the coil was not encapsulated with Parylene and physiological solution was in immediate contact with the coil, the immersion in the solution added a capacitance of up to 33 pF, and as a result, decreased the resonance frequency by up to 12% and  $Q$  by up to 70%, which results in a significantly decreased transmission distance. When the coil was encapsulated with Parylene, the immersion in PBS solution affected the coil’s electrical properties clearly less than the coil that was not encapsulated, depending on the thickness of Parylene. When a thicker Parylene encapsulation was used, the influence of surrounding physiological medium was less significant. When the Parylene encapsulation was  $6.3 \mu\text{m}$  thick, the changes in resonance frequency and  $Q$  due to the physiological medium were only 1.1% and 0.07%, respectively. Thus, the Parylene encapsulation not only protects electronic



components for the neural interface device, but also keeps the electrical properties of the coil unaffected by surrounding medium in a physiological environment.

In our previous study [7], [8], Parylene as encapsulation for active implants was characterized including long-term material stability, showing that Parylene encapsulation was stable over about one-and-half years by measuring leakage current and impedance spectroscopy using planar interdigitated electrode (IDE) test structures. On the other hand, this paper focuses on the influence of physiological medium on inductive coupling and wireless transmission, which has remained unexplored before this study although there have been many implantable devices developed employing inductive transmission. For the long-term effects of biological medium on inductive coupling are certainly of greatest interest in ultimate applications of such devices, investigations on this issue are currently being conducted by the authors' group. This set of studies includes long-term data of changes in electrical properties of the coil due to the exposure to a simulated physiological environment, changes in resonance frequency and quality factor of the coil when it is connected with an SMD capacitor and when it is integrated with IC and UEA. In all cases, the coil assemblies are coated with Parylene in various thicknesses of 1 to 20  $\mu\text{m}$ . This study will provide information on long-term influences of soaking the encapsulated device in physiological medium in a systematic manner, enabling to identify potential failure modes of the device. Parallel to the neural interface device presented in this paper, which consists of individual components stacking on each other [4], we are pursuing an alternative design employing a lid made of silicon to protect electronic components inside, and therefore, provide a better protection and hermetic sealing to the device. The concept of this approach was presented in [28] and [29].

Another factor that needs to be accounted for in achieving an optimized inductive power link is the electrical connection of the coil to the load. The additional capacitance and resistance involved in the connection of the coil and the load have to be considered. The IN14 chip added an additional capacitance of about 40–50 pF parallel to the coil, and the thin-film interconnection traces deposited on the UEA added an additional resistive loss in the coil connection, resulting in a decreased  $Q$  for the coil. The Au and Cu coils optimized taking all these factors into account demonstrated a maximum transmission distance of 17 mm for Cu coil and 18 mm for Au coil in the air. From the results of this study, it is predicted that the resonance frequency and  $Q$  of the coil will not be affected even if the coil is immersed in PBS solution, when a Parylene encapsulation of greater than 6  $\mu\text{m}$  is used. In this case, the transmission distance achieved through air would also be achievable in an implanted physiological environment.

Although we investigated the influence of system packaging and Parylene encapsulation for a specific type of neural interface based on the UEA, the results reported here can be useful for other types of implantable devices that are powered wirelessly through inductive coupling or contain integrated electronic circuitry. This paper will provide information on the effect of not only Parylene but also other polymeric encapsulants such as silicones, polyimides, or epoxies on inductively coupled power

link as they have similar electrical conductivities and dielectric constants that affect the electrical characteristics of the implant coil. A current on-going study by the authors' group includes measurements of changes in electrical properties of the coil coated with Parylene and other polymeric materials that can potentially be used as device encapsulation, which will give a more general set of knowledge on the effects of encapsulation materials and wireless transmission for different materials and different environmental conditions.

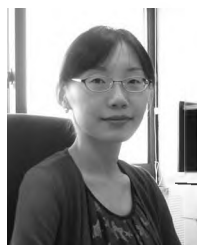
#### ACKNOWLEDGMENT

The authors acknowledge L. Boylston of IEC Company (Conway, SC) for manufacturing the coils, and would like to thank K. Nelson for Parylene encapsulation and R. Kier for providing the programs to record impedances.

#### REFERENCES

- [1] F. Solzbacher, R. Harrison, R. A. Normann, L. Rieth, S. Chakravarty, J.-M. Hsu, M. Klein, H. Oppermann, M. Toepper, and R. Hahn, "A next generation chronically implantable wireless neural interface," presented at the *NIH/NINDS Annu. Neural Interfaces Workshop*, Bethesda, MD, Sep. 7–9, 2005 (invited paper).
- [2] F. Solzbacher, R. Harrison, R. Normann, H. Oppermann, M. Klein, K. P. Koch, S. Kammer, A. Ramachandran, and S. Kim, "Integrated neural interface arrays for neuroprosthetics applications," in *Proc. 1st Annu. Meeting Amer. Acad. Nanomed.*, Aug. 15–16, 2005, pp. 250–251.
- [3] M. Töpper, M. Klein, K. Buschick, V. Glaw, K. Orth, O. Ehrmann, M. Hutter, H. Oppermann, K.-F. Becker, T. Braun, F. Ebling, H. Reichl, S. Kim, P. Tathireddy, S. Chakravarty, and F. Solzbacher, "Biocompatible hybrid flip chip microsystem integration for next generation wireless neural interfaces," in *Proc. 56th Electron. Compon. Technol. Conf. (ECTC'06)*, San Diego, CA, May 30–Jun. 2, 2006, pp. 705–708.
- [4] S. Kim, R. Bhandari, M. Klein, S. Negi, L. Rieth, P. Tathireddy, M. Toepper, H. Oppermann, and F. Solzbacher, "Integrated wireless neural interface based on the Utah electrode array," *Biomed. Microdevices*, vol. 11, no. 2, pp. 453–466, 2009.
- [5] S. Kim, K. Zoschke, M. Klein, D. Black, K. Buschick, M. Toepper, P. Tathireddy, R. Harrison, H. Oppermann, and F. Solzbacher, "Switchable polymer based thin film coils as a power module for wireless neural interfaces," *Sens. Actuators A*, vol. 136, pp. 467–474, 2007.
- [6] J.-M. Hsu, P. Tathireddy, L. Rieth, R. A. Normann, and F. Solzbacher, "Characterization of a-SiC<sub>x</sub>H thin films as an encapsulation material for integrated silicon based neural interface devices," *Thin Solid Films*, vol. 516, no. 1, pp. 34–41, 2007.
- [7] J.-M. Hsu, L. Rieth, S. Kammer, M. Orthner, and F. Solzbacher, "Influence of thermal and deposition processes on the surface morphology, crystallinity, and adhesion of Parylene-C," *Sens. Mater.*, vol. 20, no. 2, pp. 071–086, 2008.
- [8] J.-M. Hsu, L. Rieth, R. A. Normann, P. Tathireddy, and F. Solzbacher, "Hermetic encapsulation of an integrated neural interface device with Parylene-C," *IEEE Trans. Biomed. Eng.*, vol. 56, no. 1, pp. 23–29, Jan. 2009.
- [9] T. Kim, P. R. Troyk, and M. Bak, "Active floating micro electrode arrays (AFMA)," in *Proc. 28th IEEE EMBS Annu. Int. Conf.*, Aug. 30–Sep. 3, 2006, pp. 2807–2810.
- [10] J. E. Anderson, V. Markovac, and P. R. Troyk, "Polymer encapsulants for microelectronics: Mechanisms for protection and failure," *IEEE Trans. Compon., Hybrids, Manuf. Technol.*, vol. 11, no. 1, pp. 152–158, Mar. 1988.
- [11] S. F. Cogan, D. J. Edell, A. A. Guzelian, Y. P. Liu, and R. Edell, "Plasma enhanced chemical vapor deposited silicon carbide as an implantable dielectric coating," *J. Biomed. Mater. Res. A*, vol. 67, pp. 856–867, 2003.
- [12] X. Xiao, J. Wang, C. Liu, J. A. Carlisle, B. Mech, R. Greenberg, D. Guven, R. Freda, M. S. Humayun, J. Weiland, and O. Auciello, "In vitro and in vivo evaluation of ultrananocrystalline diamond for coating of implantable retinal microchips," *J. Biomed. Mater. Res. B, Appl. Biomater.*, vol. 77, pp. 273–281, 2006.

- [13] S. Takeuchi, D. Ziegler, Y. Yoshida, K. Mabuchi, and T. Suzuki, "Parylene flexible neural probes integrated with microfluidic channels," *Lab Chip*, vol. 5, pp. 519–523, 2005.
- [14] P. A. Stupar and A. P. Pisano, "Silicon, parylene, and silicon/parylene micro-needles for strength and toughness," in *Proc. 11th Int. Conf. Solid-State Sens. Actuators*, Munich, Germany, 2001, pp. 1386–1389.
- [15] E. M. Schmidt, J. S. McIntosh, and M. J. Bak, "Long-term implants of Parylene-C coated microelectrodes," *Med. Biol. Eng. Comput.*, vol. 26, pp. 96–101, 1988.
- [16] K. J. James, "An analysis of insulating material used to encapsulate silicon-based microelectrode arrays," Ph.D. dissertation, Univ. Utah, Salt Lake City, 1995.
- [17] T. Stieglitz, "Biomedical microimplants for sensory and motor neuroprostheses," in *Proc. ISCAS 2006*, pp. 2189–2192.
- [18] D. J. Edell, "Insulating biomaterials," NIH/NINDS Neural Prosthesis Program Rep., Bethesda, MD, Contract I-NS-3-2301, 1993.
- [19] K. Najafi, "Micropackaging technologies for integrated microsystems: Applications to MEMS and MOEMS," presented at the *SPIE Micromachining Microfabrication Symp.*, San Jose, CA, 2003.
- [20] B. H. Stark and K. Najafi, "An ultra-thin hermetic package utilizing electroplated gold," in *Proc. Dig. 11th IEEE Int. Conf. Solid-State Sens. Actuators (Transducers 2001)*, pp. 194–197.
- [21] R. R. Harrison, "Designing efficient inductive power links for implantable devices," in *Proc. 2007 IEEE Intl. Symp. Circuits Syst. (ISCAS 2007)*, New Orleans, LA, pp. 2080–2083.
- [22] P. House, internal communication, University of Utah, Salt Lake City, 2006.
- [23] S. Kim, O. Scholz, and F. Solzbacher "Design and optimization of planar microcoils used in implantable telemetry systems," submitted for publication.
- [24] R. R. Harrison, P. T. Watkins, R. J. Kier, D. J. Black, R. O. Lovejoy, R. A. Normann, and F. Solzbacher, "Design and testing of an integrated circuit for multi-electrode neural recording," in *Proc. 20th Int. Conf. VLSI Des. (VLSID 2007)*, Bangalore, India, Jan. 6–10, 2007, pp. 907–912.
- [25] R. R. Harrison, P. T. Watkins, R. J. Kier, R. O. Lovejoy, D. J. Black, B. Greger, and F. Solzbacher, "A low-power integrated circuit for a wireless 100-electrode neural recording system," *IEEE J. Solid-State Circuits*, vol. 42, no. 1, pp. 123–133, Jan. 2007.
- [26] R. R. Harrison, R. J. Kier, C. A. Chestek, V. Gilja, P. Nuyujukian, S. I. Ryu, B. Greger, F. Solzbacher, and K. V. Shenoy, "Wireless neural signal acquisition with single low-power integrated circuit," in *Proc. 2008 IEEE Int. Symp. Circuits Syst. (ISCAS 2008)*, Seattle, WA, May 18–21, pp. 1748–1751.
- [27] C. A. Chestek, V. Gilja, R. J. Kier, P. Nuyujukian, S. I. Ryu, F. Solzbacher, R. Harrison, and K. V. Shenoy, "HermesC: RF wireless low-power neural recording system for freely-behaving primates," in *Proc. 2008 IEEE Int. Symp. Circuits Syst. (ISCAS 2008)*, Seattle, WA, May 18–21, pp. 1752–1755.
- [28] S. Kim, M. Wilke, M. Klein, M. Toepper, and F. Solzbacher, "Electromagnetic compatibility of two novel packaging concepts of an inductively powered neural interface," in *Proc. 3rd Int. IEEE EMBS Conf. Neural Eng.*, Kohala Coast, HI, May 2–5, 2007, pp. 434–437.
- [29] M. Wilke, M. Töpper, S. Kim, M. Klein, K.-H. Drüe, J. Müller, M. Wiemer, V. Glaw, H. Oppermann, F. Solzbacher, and H. Reichl, "Development of a capping process based on Si and LTCC for a wireless neuroprosthetic implant," presented at the *NIH/NINDS Neural Interfaces Workshop*, Bethesda, MD, Aug. 21–23, 2006.



**Sohee Kim** (M'07) received the B.S. and M.S. degrees in mechanical engineering from Korea Advanced Institute of Science and Technology, Daejeon, Korea in 1998 and 2000, respectively, and the Dr.-Ing. (Ph.D.) degree in electrical engineering from the University of Saarland, Saarbruecken, Germany, in 2005.

From 2001 to 2005, she was a Research Engineer with the Fraunhofer Institute for Biomedical Engineering, St. Ingbert, Germany. From 2006 to 2009, she was Postdoctoral Fellow in the Department of Electrical and Computer Engineering, University of

Utah, Salt Lake City, where she was also a Research Assistant Professor. She is currently an Assistant Professor in the Department of Mechatronics, Gwangju Institute of Science and Technology, Gwangju, Korea. Her research interests include neural interfaces, microelectrodes, wireless powering, and telemetry for implantable systems including electromagnetic and thermal aspects of such implants.



**Reid R. Harrison** (S'98-M'00) was born in DeFuniak Springs, FL. He received the B.S. degree in electrical engineering from the University of Florida, Gainesville, in 1994, and the Ph.D. degree from the California Institute of Technology, Pasadena, in 2000.

In 2000, he joined the University of Utah, Salt Lake City, where he is currently an Associate Professor of electrical and computer engineering and an Adjunct Associate Professor of bioengineering. His current research interests include low-power analog and mixed-signal CMOS circuit design, integrated

electronics for neural interfaces and other biomedical devices, and biologically inspired computation.

Dr. Harrison was a member of the technical program committees of the International Solid-State Circuits Conference (ISSCC) and the IEEE International Symposium on Circuits and Systems. He received the National Science Foundation CAREER Award in 2002 and the Jack Raper Award for Outstanding Technology Directions Paper from the ISSCC in 2006.



**Florian Solzbacher** (M'04) received the M.Sc.E.E. degree from the Technical University Berlin, Berlin, Germany, in 1997, and the Ph.D. degree from the Technical University Ilmenau, Ilmenau, Germany, in 2003.

He is the Director of Microsystems Laboratory and the Utah Nanofabrication Facility, University of Utah, Salt Lake City, where he is also a Co-Director of Utah Nanotechnology Institute, the President of Blackrock Microsystems, and holds faculty appointments in electrical and computer engineering,

materials science and bioengineering. He is a Co-Founder of several companies such as Blackrock Microsystems, First Sensor Technology, and NFocus. He has authored or coauthored more than 100 journal and conference publications, five book chapters, and holds 16 pending patents. His current research interests include harsh environment microsystems and materials, including implantable and wireless microsystems for biomedical and healthcare applications, and high-temperature and harsh-environment-compatible microsensors.

Dr. Solzbacher is the Chairman of the German Association for Sensor Technology AMA. He is a member of a number of company and public private partnership advisory boards.